

# Electronic structure of SrPt<sub>4</sub>Ge<sub>12</sub>: a combined photoelectron spectroscopy and band structure study

H. Rosner,<sup>1</sup> J. Gegner,<sup>2</sup> D. Regesch,<sup>2</sup> W. Schnelle,<sup>1</sup> R. Gumeniuk,<sup>1</sup> A. Leithe-Jasper,<sup>1</sup> H. Fujiwara,<sup>2</sup> T. Hauptprich,<sup>2</sup> T. C. Koethe,<sup>2</sup> H.-H. Hsieh,<sup>3</sup> H.-J. Lin,<sup>4</sup> C. T. Chen,<sup>4</sup> A. Ormeci,<sup>1</sup> Yu. Grin,<sup>1</sup> and L. H. Tjeng<sup>2</sup>

<sup>1</sup> *Max-Planck-Institut für Chemische Physik fester Stoffe, Nöthnitzer Straße 40, 01187 Dresden, Germany*

<sup>2</sup> *II. Physikalisches Institut, Universität zu Köln, Zùlpicher Straße 77, 50937 Köln, Germany*

<sup>3</sup> *Chung Cheng Institute of Technology, National Defense University, Taoyuan 335, Taiwan*

<sup>4</sup> *National Synchrotron Radiation Research Center (NSRRC), 101 Hsin-Ann Road, Hsinchu 30077, Taiwan*

(Dated: November 13, 2018)

We present a combined study of the electronic structure of the superconducting skutterudite derivative SrPt<sub>4</sub>Ge<sub>12</sub> by means of X-ray photoelectron spectroscopy and full potential band structure calculations including an analysis of the chemical bonding. We establish that the states at the Fermi level originate predominantly from the Ge 4*p* electrons and that the Pt 5*d* shell is effectively full. We find excellent agreement between the measured and the calculated valence band spectra, thereby validating that band structure calculations in combination with photoelectron spectroscopy can provide a solid basis for the modeling of superconductivity in the compounds MPt<sub>4</sub>Ge<sub>12</sub> (*M* = Sr, Ba, La, Pr) series.

PACS numbers: 71.20.Eh, 79.60.-i

## I. INTRODUCTION

Compounds with crystal structures featuring a rigid covalently bonded framework enclosing differently bonded guest atoms attracted much attention in the last decade. In particular the skutterudite and clathrate families have been investigated in depth, and a fascinating diversity of physical phenomena is observed, many of which are due to subtle host-guest interactions. Among the skutterudites they range from magnetic ordering to heavy-fermion and non-Fermi liquids, superconductivity, itinerant ferromagnetism, half-metallicity, and good thermoelectric properties.<sup>1,2,3,4</sup> Superconductivity of conventional<sup>5,6,7</sup> and heavy-fermion type is found in skutterudites with *T<sub>c</sub>*'s up to 17 K.<sup>8,9,10</sup>

The formula of the filled skutterudites, being derived from the mineral CoAs<sub>3</sub>, is given by *M<sub>y</sub>T<sub>4</sub>X<sub>12</sub>*, with *M* a cation, *T* a transition metal, and *X* usually a pnictogen (P, As, or Sb). The *M* atoms reside in large icosahedral cages formed by [*TX*<sub>6</sub>] octahedra. A new family of superconducting skutterudites MPt<sub>4</sub>Ge<sub>12</sub> (*M* = Sr, Ba, La, Pr, Th) has been reported recently.<sup>11,12,13</sup> With trivalent La and Pr, *T<sub>c</sub>*'s up to 8.3 K are observed. The compounds with the divalent cations Sr and Ba have lower *T<sub>c</sub>*'s around 5.0 K.<sup>11,12</sup>

Band structure calculations predict that the electronic density of states (DOS) close to the Fermi level *E<sub>F</sub>* is determined by Ge-4*p* states in all MPt<sub>4</sub>Ge<sub>12</sub> materials.<sup>11,12,14</sup> The position of *E<sub>F</sub>* is adjusted by the electron count on the polyanionic host structure. This leads to the situation that the band structure at *E<sub>F</sub>* can be shifted in an almost rigid-band manner by “doping” of the polyanion, which can be achieved either by charge transfer from the guest *M* or by internal substitution of the transition metal *T*. Recently, this principle was demonstrated on the Pt-by-Au substitu-

tion in BaPt<sub>4-x</sub>Au<sub>x</sub>Ge<sub>12</sub>: while BaPt<sub>4</sub>Ge<sub>12</sub> has a calculated DOS of 8.8 states/(eV f.u.), at the composition BaPt<sub>3</sub>AuGe<sub>12</sub> the DOS is enhanced to 11.5 states/(eV f.u.).<sup>15</sup> Experimentally, an increase of the superconducting *T<sub>c</sub>* from 5.0 K to 7.0 K.<sup>15</sup> was observed. The rigid-band shift of the DOS peak at *E<sub>F</sub>* with gold substitution is due to the Pt(Au) 5*d* electrons which, according to band structure calculations, lie rather deep below *E<sub>F</sub>* and provide only a minor contribution to the DOS at *E<sub>F</sub>*.<sup>15</sup>

Another prediction from the band structure calculations concerns the special role played by the Pt 5*d* states in SrPt<sub>4</sub>Ge<sub>12</sub> for the chemical bonding. It is known, assuming two-center-two-electron bonds within the *T-X* framework for the binary skutterudites, that 72 electrons are required for the stabilization of the [*T<sub>4</sub>X<sub>12</sub>*] formula unit.<sup>1</sup> In the case of SrPt<sub>4</sub>Ge<sub>12</sub>, the total number of *s* and *p* electrons of Sr, Pt and Ge is 2+4×2+12×4=58. To achieve the target value of 72, each Pt atom should use 3.5 *d* electrons for bonding, which would be a rather large value compared to the one *d* electron per Co atom in Co<sub>4</sub>As<sub>12</sub> (4×CoAs<sub>3</sub>).

In order to determine the electron counts for SrPt<sub>4</sub>Ge<sub>12</sub> as a characteristic for the chemical bonding, we evaluated the so-called electron localizability indicator (ELI). The combined analysis of the ELI and electron density (ED), see Figure 1, shows indeed three types of attractors in the valence region: two representing Ge-Ge bonds and one reflecting the Pt-Ge bond. No attractors were found between Sr and the framework atoms, suggesting predominantly ionic interaction here. The Ge-Ge bonds are two-electron bonds (electron counts 1.90 and 2.01), the Pt-Ge bond has a count of only 1.53 electrons, summing up to 60.18 electrons total per [Pt<sub>4</sub>Ge<sub>12</sub>] formula unit. This means that only about 0.5 *d* electrons per Pt are participating in the stabilization of the [Pt<sub>4</sub>Ge<sub>12</sub>] polyanion. Both procedures, valence electron counting

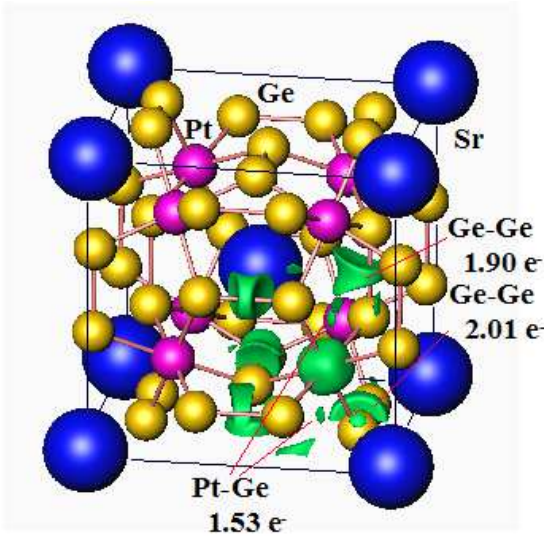


FIG. 1: Chemical bonding in  $\text{SrPt}_4\text{Ge}_{12}$ : isosurface of ELI revealing Ge-Ge and Pt-Ge bonds together with their electron counts.

and combined ELI/ED analysis yield unusual results and raise the question about the role of  $5d$  electrons of Pt in the formation of the  $\text{MPt}_4\text{Ge}_{12}$  compounds.

Up to now, no spectroscopic data are available to challenge the above mentioned band structure predictions and chemical bonding analysis. Such a validation is important since one would like to know whether band theory can provide a solid basis for the modeling of superconductivity in the  $\text{MPt}_4\text{Ge}_{12}$  ( $M = \text{Sr}, \text{Ba}, \text{La}, \text{Pr}$ ) series. We therefore set out to perform a comparative study of the valence band electronic structure of the superconducting skutterudite derivative  $\text{SrPt}_4\text{Ge}_{12}$  by means of x-ray photoelectron spectroscopy (PES) and full potential band structure calculations.

## II. METHODS

Samples were prepared by standard techniques as described in Refs. 12 and 15. Metallographic and electron microprobe tests of polished specimens detected only traces of  $\text{PtGe}_2$  ( $< 4 \text{ vol}\%$ ) and  $\text{SrPt}_2\text{Ge}_2$  ( $< 1 \text{ vol}\%$ ) as impurity phases in the sample  $\text{SrPt}_4\text{Ge}_{12}$ . EPMA confirmed the ideal composition of the target phase. The lattice parameter is  $8.6509(5) \text{ \AA}$ , as reported earlier.<sup>12</sup> For the cation position full occupancy was derived from full-profile crystal structure refinements of powder XRD data, which are in good agreement with single crystal data obtained in Ref. 11.

The PES experiments were performed at the Dragon beamline of the NSRRC in Taiwan using an ultra-high vacuum system (pressure in the low  $10^{-10}$  mbar range) which is equipped with a Scienta SES-100 electron energy analyzer. The photon energy was set to 700 eV and to 190 eV. The latter energy is close to the Cooper minimum in the photo-ionization cross section of the Pt  $5d$  valence

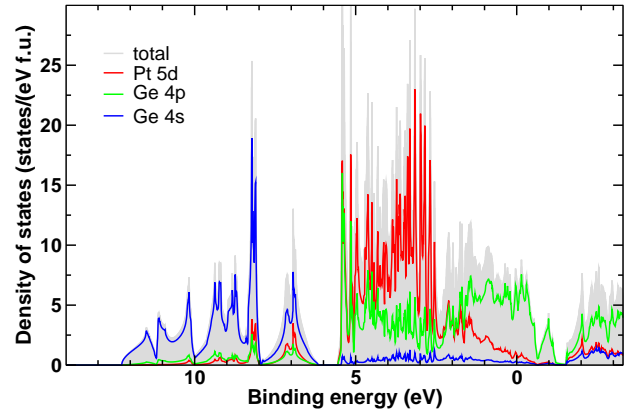


FIG. 2: Calculated total and atom resolved partial electronic density of states of  $\text{SrPt}_4\text{Ge}_{12}$ . The Fermi level is at zero energy.

shell.<sup>16</sup> The overall energy resolution was set to 0.35 eV and 0.25 eV, respectively, as determined from the Fermi cut-off in the valence band of a Au reference which was also taken as the zero of the binding energy scale. The  $4f_{7/2}$  core level of Pt metal was used as an energy reference, too. The reference samples were scraped *in-situ* with a diamond file. The polycrystalline  $\text{SrPt}_4\text{Ge}_{12}$  sample with dimensions of  $2 \times 2 \times 3 \text{ mm}^3$  was cleaved *in-situ* exposing a shiny surface and measured at room temperature at normal emission.

Electronic structure calculations within the local density approximation (LDA) of DFT were employed using the full-potential local-orbital code FPLO (version 5.00-19).<sup>17</sup> In the full-relativistic calculations, the exchange and correlation potential of Perdew and Wang<sup>18</sup> was used. As the basis set, Sr( $4s, 4p, 5s, 5p, 4d$ ), Pt ( $5s, 5p, 6s, 6p, 5d$ ), and Ge ( $3d, 4s, 4p, 4d$ ) states were employed. Lower-lying states were treated as core. A very dense  $k$ -mesh of 1256 points in the irreducible part of the Brillouin zone ( $30 \times 30 \times 30$  in the full zone) was used to ensure accurate density of states (DOS) information.

The electron localizability indicator was evaluated according to Ref. 19 with an ELI/ELF module implemented within the FPLO program package.<sup>20</sup> The topology of ELI was analyzed using the program Basin<sup>21</sup> with consecutive integration of the electron density in basins, which are bound by zero-flux surfaces in the ELI gradient field. This procedure, similar to the one proposed by Bader for the electron density<sup>22</sup> allows to assign an electron count for each basin, providing fingerprints of direct (covalent) interactions.

Figure 2 shows the calculated DOS for  $\text{SrPt}_4\text{Ge}_{12}$  ( $E_F$  is at zero binding energy). The valence band is almost exclusively formed by Pt and Ge states. The low and featureless Sr DOS indicates that it plays basically the role of a charge reservoir. Further inspection of the DOS shows that the high-lying states between about 6 and 12 eV binding energies originate predominantly from Ge  $4s$  electrons, whereas the lower lying part of the valence band is formed by Pt  $5d$  and Ge  $4p$  states. The Pt  $5d$

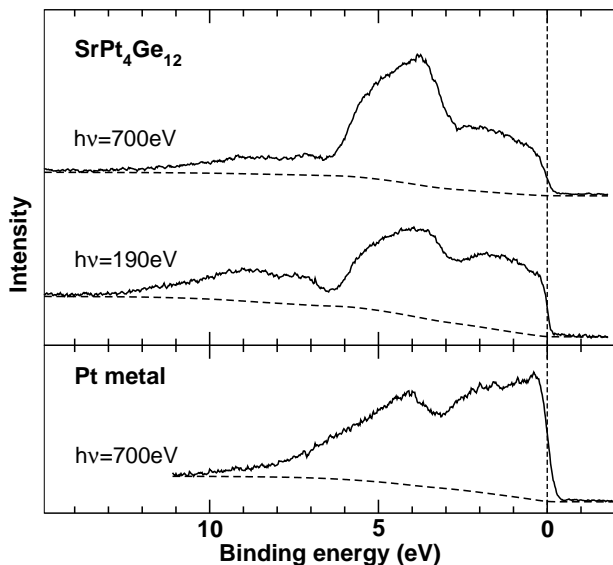


FIG. 3: Valence band photoemission spectra of  $\text{SrPt}_4\text{Ge}_{12}$  taken with a photon energy of  $h\nu = 700$  eV (upper panel) and 190 eV (middle panel). As reference, the valence band spectrum of elemental Pt metal taken at  $h\nu = 700$  eV is also given (bottom panel). The spectra are normalized with respect to their integrated intensities after subtracting an integral background indicated by the dashed curves.

states essentially form a narrow band complex of approximately 3 eV band width centered at about 4 eV binding energy. Our calculated DOS is in good agreement with the previous results of Bauer et al.<sup>11</sup>

Figure 3 displays the valence band photoemission spectra of  $\text{SrPt}_4\text{Ge}_{12}$ , taken with a photon energy of  $h\nu = 700$  eV (upper panel) and 190 eV (middle panel), together with the reference spectrum of elemental Pt metal (bottom panel). The spectra are normalized to their integrated intensities, after an integral background has been subtracted to account for inelastic scattering. All spectra show a clear cut-off at  $E_F$  (zero binding energy) consistent with the systems being good metals. It is of no surprise that the 700 eV spectrum of  $\text{SrPt}_4\text{Ge}_{12}$  is very much different from that of Pt since they are different materials. More interesting is that there are also differences between the 700 eV and 190 eV spectra of  $\text{SrPt}_4\text{Ge}_{12}$  itself. This is caused by differences in the photon energy dependence of the photo-ionization cross-section of the relevant subshells forming the valence band, in this case, the Ge 4s, 4p, and Pt 5d.<sup>16</sup> In fact, we chose those 190 eV and 700 eV photon energies in order to make optimal use of the cross-section effects for identifying the individual contributions of the Ge and Pt states to the valence band as we will show in the next sections. In particular, at 700 eV the Pt 5d cross-section is calculated to be a factor 3.9 larger than that of the Ge 4p, while at 190 eV (close to the Cooper minimum for the Pt 5d) it is equal or even slightly smaller, i.e. a factor 0.92, see Table I. In other words, the 700 eV spectra is dominated by the Pt 5d contribution while at 190 eV the contributions become

TABLE I: Calculated photo-ionization cross-sections per electron ( $\sigma$  in Mb/e) for the Pt 5d, Ge 4p and Ge 4s subshells, from Yeh and Lindau.<sup>16</sup>

$h\nu$ (eV)	$\sigma^{Pt5d}$	$\sigma^{Ge4p}$	$\sigma^{Ge4s}$	$\sigma^{Pt5d}/\sigma^{Ge4p}$	$\sigma^{Pt5d}/\sigma^{Ge4s}$
190	0.0099	0.0108	0.021	0.92	0.47
700	0.0074	0.0019	0.0030	3.9	2.5

comparable.

The intensity  $I$  of a normalized spectrum as depicted in Figure 3 is built up from the Pt 5d, Ge 4p and Ge 4s partial DOS ( $\rho$ ), weighted with their respective photo-ionization cross-sections ( $\sigma$ ). This is formulated in equations 1 and 2 which take into account that the cross-sections at 190 eV photon energy are different from those at 700 eV, respectively. The proportionality factors  $c_{190}$  and  $c_{700}$ , respectively, also enter here since the absolute values for the photon flux and the transmission efficiency of the electron energy analyzer are not known. In addition, the constants  $\alpha$ ,  $\beta$ , and  $\gamma$  are introduced to express the non-uniqueness in the calculation of the weight of the Pt 5d, Ge 4p, and Ge 4s DOS, respectively, since these depend (somewhat) on which calculational method has been used.

$$I_{190} = c_{190}[\sigma_{190}^{Pt5d} \alpha \rho^{Pt5d} + \sigma_{190}^{Ge4p} \beta \rho^{Ge4p} + \sigma_{190}^{Ge4s} \gamma \rho^{Ge4s}] \quad (1)$$

$$I_{700} = c_{700}[\sigma_{700}^{Pt5d} \alpha \rho^{Pt5d} + \sigma_{700}^{Ge4p} \beta \rho^{Ge4p} + \sigma_{700}^{Ge4s} \gamma \rho^{Ge4s}] \quad (2)$$

Using the predictions of the band structure calculations as a guide, we notice that the Ge 4s states hardly give a contribution in the energy range between the Fermi level and 6 eV binding energy. In this range, i.e. most relevant for the properties, the valence band seems to be determined mostly by the Pt 5d and Ge 4p states. We now analyze the experimental spectra along these lines. Using equations (1) and (2), we can experimentally extract the Pt 5d and Ge 4p DOS as follows:

$$\rho^{Pt5d} \sim I_{700} - A \times I_{190} \quad (3)$$

$$\rho^{Ge4p} \sim I_{190} - B \times I_{700} \quad (4)$$

with  $A = (c_{700}/c_{190}) \times (\sigma_{700}^{Ge4p}/\sigma_{190}^{Ge4p})$  and  $B = (c_{190}/c_{700}) \times (\sigma_{190}^{Pt5d}/\sigma_{700}^{Pt5d})$ . While the cross-sections  $\sigma$  can be readily obtained from Table I, it would be an enormous task to determine (experimentally) the ratio between  $c_{700}$  and  $c_{190}$ . Thus, since it is difficult to obtain directly an estimate for  $A$  and  $B$ , we use the product  $AB$  given by  $(\sigma_{190}^{Pt5d}/\sigma_{190}^{Ge4p})/(\sigma_{700}^{Pt5d}/\sigma_{700}^{Ge4p})$ , which can be calculated from Table I to be about  $0.92/3.9 = 0.24$ . Therefore, we vary the values for  $A$  and  $B$  under the constraint that  $AB = 0.24$ , searching for difference spectra which reproduce both the Pt 5d and the Ge 4p DOS as obtained by the band structure calculations.

We find good results for  $A = 0.6$  and  $B = 0.4$  as displayed in Figures 4 and 5. Focusing first at Figure 4 in

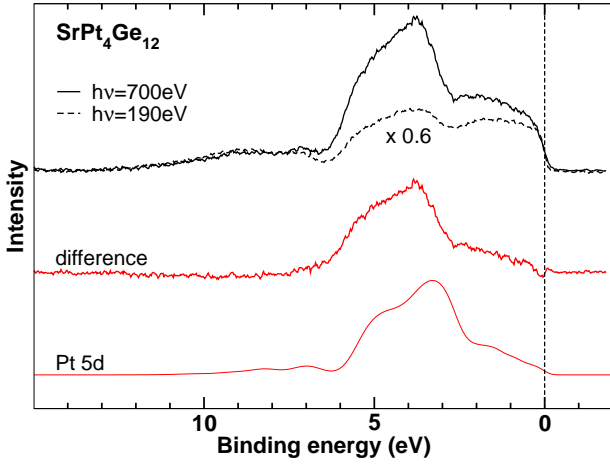


FIG. 4: (Color online) Normalized and background-corrected valence band photoemission spectra of  $\text{SrPt}_4\text{Ge}_{12}$  taken with a photon energy of  $h\nu = 700$  eV (black solid line) and 190 eV (black dashed line). The 190 eV spectrum has been rescaled with a factor 0.6 (see text). The difference spectrum (red

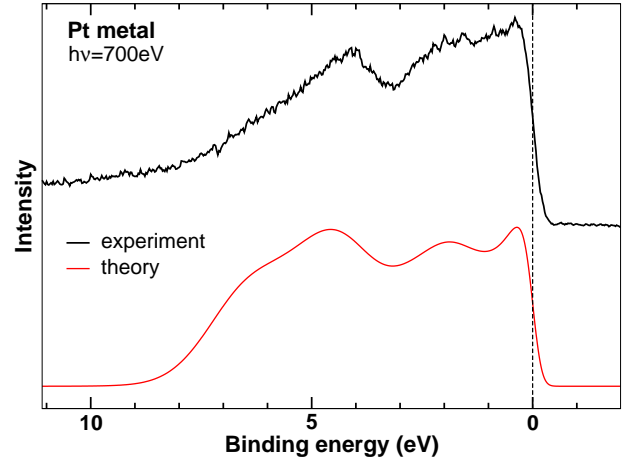


FIG. 6: (Color online) Valence band photoemission spectrum of elemental Pt metal taken with a photon energy of  $h\nu = 700$  eV (black-solid line) and the calculated Pt  $5d$  DOS (red-solid line).

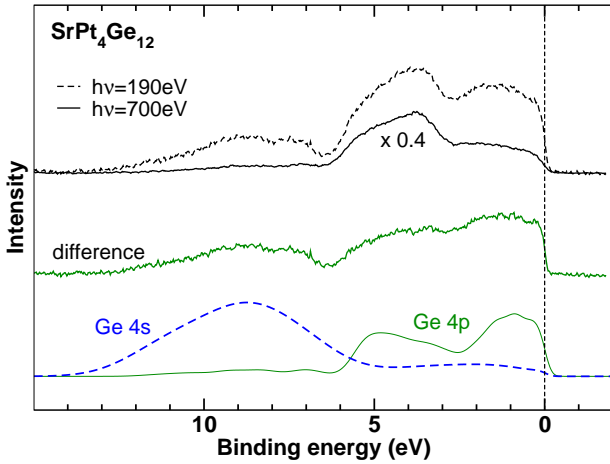


FIG. 5: (Color online) Normalized and background-corrected valence band photoemission spectra of  $\text{SrPt}_4\text{Ge}_{12}$  taken with a photon energy of  $h\nu = 190$  eV (black dashed line) and 700 eV (black solid line). The 700 eV spectrum has been rescaled with a factor 0.4. The difference spectrum (green solid line) is compared to the calculated Ge  $4p$  DOS (green thin line) and Ge  $4s$  DOS (blue dashed line).

which the rescaled 190 eV spectrum is subtracted from the 700 eV one, we can observe that the difference spectrum resembles very much that of the calculated Pt  $5d$  DOS. Here the latter has been broadened to account for the experimental resolution and lifetime effects. Interestingly, the main Pt intensity is positioned at around 3-6 eV binding energies and its weight near the  $E_F$  region is very small. The experiment fully confirms this particular aspect of the theoretical prediction, which is important for the modeling of the superconducting properties as discussed above. We would like to note that the main peak of the calculated Pt  $5d$  DOS is positioned at a some-

what lower binding energy than that of the experimental difference spectrum. Similar small deviations have been observed in other intermetallic materials<sup>23,24</sup> and can be attributed to the inherent limitations of mean-field methods like the LDA to calculate the dynamic response of a system.

Figure 5 shows the difference of the spectrum taken at 190 eV and the rescaled spectrum at 700 eV. This experimental difference spectrum reveals structures which can be divided into two major energy regions: the first region extends from 0 to 6 eV binding energy, and the second from 6 to 12 eV. For the first region we can make a comparison with the calculated Ge  $4p$  DOS, since the calculated Ge  $4s$  contribution is negligible as explained above. We obtain a very satisfying agreement between the experiment and theory for the Ge  $4p$  states. In particular, we would like to point out that the experiment confirms the strong presence of the Ge  $4p$  states in the vicinity of the Fermi level  $E_F$ . Looking now at the second region, we see that the calculated Ge  $4s$  also reproduces nicely the experimental difference spectrum. Here we remark that the calculated Ge  $4p$  has a negligible contribution in this region.

As a further check we also perform a comparison between the experimental photoemission spectrum of elemental Pt metal and the corresponding calculated Pt  $5d$  DOS. The result is shown in Figure 6. Also here we find satisfying agreement between experiment and theory. The Pt  $5d$  states range from 9 eV binding energy all the way up to  $E_F$ . Clearly, the high Fermi cut-off in Pt metal is formed by these Pt  $5d$  states, in strong contrast to the  $\text{SrPt}_4\text{Ge}_{12}$  case.

Figure 7 shows the Pt  $4f$  core levels of  $\text{SrPt}_4\text{Ge}_{12}$  (top) and elemental Pt metal (bottom). The spectra exhibit the characteristic spin-orbit splitting giving the  $4f_{5/2}$  and  $4f_{7/2}$  peaks. For  $\text{SrPt}_4\text{Ge}_{12}$ , the peak positions for the  $4f_{5/2}$  and  $4f_{7/2}$  are 75.4 and 72.1 eV binding energy, respectively. For Pt metal, the values are 74.4 and 71.1 eV,

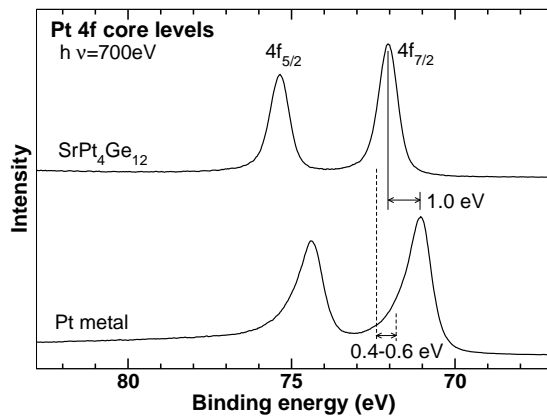


FIG. 7: Pt  $4f$  core level photoemission spectra of  $\text{SrPt}_4\text{Ge}_{12}$  (top) and elemental Pt metal (bottom). Solid vertical lines represent the peak positions of the  $4f_{7/2}$  levels, dashed vertical lines the center of gravity positions (see text).

respectively. The spin orbit splitting is thus 3.3 eV for both materials. This compares well with the calculated spin-orbit splitting of about 3.45 eV for both compounds from the LDA calculations.

Remarkable is that the  $\text{SrPt}_4\text{Ge}_{12}$   $4f$  peaks are shifted by 1 eV to higher binding energies in comparison to those of Pt metal. Similar shifts have also been observed in other noble metal intermetallic compounds,<sup>23,24,25</sup> indicating a more dilute electron density around the noble metal sites. To compare this chemical shift to LDA calculations, one has to take into account that LDA does not incorporate many body effects of the final state, manifesting in the asymmetric line shape of the spectra as we will discuss below in more detail. But it can be shown<sup>26</sup> that final state effects do not alter the average energy of the spectrum. If we determine the center of gravity of the

$4f_{7/2}$ , we find a binding energy of 72.4 eV for  $\text{SrPt}_4\text{Ge}_{12}$  and  $71.9 \pm 0.2$  eV (indicated by dashed lines in Figure 7) for Pt metal, resulting in a chemical shift of 0.4 eV to 0.6 eV. This agrees well with the shift obtained from our band structure calculations which amounts to 0.43 eV.

One can clearly observe that the line shape of the core levels in  $\text{SrPt}_4\text{Ge}_{12}$  is narrower and not as asymmetric as in the case of Pt metal. An asymmetry in the line shape is caused by the presence of electron-hole pair excitations upon the creation of the core hole, i.e. screening of the core hole by conduction band electrons, and can be well understood in terms of the Doniach-Sunjic theory.<sup>27</sup> The strong asymmetry of the  $4f$  of Pt metal can therefore be taken as an indication for the high DOS with Pt character at  $E_F$ .<sup>28</sup> The rather symmetric line shape of the  $4f$  of  $\text{SrPt}_4\text{Ge}_{12}$ , on the other hand, indicates very low DOS at  $E_F$ . All this confirms the results of the valence band measurements: the main intensity of the Pt  $5d$  band is at 3-6 eV binding energies, strongly reducing its weight at  $E_F$ .

In conclusion, we find excellent agreement between the measured photoemission spectra and the LDA band structure calculations for  $\text{SrPt}_4\text{Ge}_{12}$ . This confirms the picture of the chemical bonding analysis yielding rather deep lying Pt  $5d$  states which only partially form covalent bands with the Ge  $4p$  electrons. In turn, the states at the Fermi level that are relevant for the superconducting behavior of this compound can be firmly assigned to Ge  $4p$  electrons. This study provides strong support that band theory is a good starting point for the understanding of the electronic structure of the  $M\text{Pt}_4\text{Ge}_{12}$  ( $M = \text{Sr, Ba, La, Pr, Th}$ ) material class, and is thus of valuable help in the search for new compositions with higher superconducting transition temperatures.

- 
- <sup>1</sup> C. Uher, *Semiconductors and Semimetals* **68**, 139 (2001).
  - <sup>2</sup> B. C. Sales, *Handbook on the Physics and Chemistry of Rare Earths* (Elsevier, Amsterdam, 2003), vol. 33, chap. 211, pp. 1–34.
  - <sup>3</sup> A. Leithe-Jasper, W. Schnelle, H. Rosner, N. Senthilkumar, A. Rabis, M. Baenitz, A. Gippius, E. Morozova, J. A. Mydosh, and Yu. Grin, *Phys. Rev. Lett.* **91**, 037208 (2003), erratum: **93**, 089904 (2004).
  - <sup>4</sup> G. S. Nolas, D. T. Morelli, and T. Tritt, *Ann. Rev. Mater. Sci.* **29**, 89 (1999).
  - <sup>5</sup> G. Meisner, *Physica B+C* **108**, 763 (1981).
  - <sup>6</sup> H. Kawaji, H.-o. Horie, S. Yamanaka, and M. Ishikawa, *Phys. Rev. Lett.* **74**, 1427 (1995).
  - <sup>7</sup> K. Tanigaki, T. Shimizu, K. M. Itoh, J. Teraoka, Y. Moritomo, and S. Yamanaka, *Nature Mater.* **2**, 653 (2003).
  - <sup>8</sup> E. D. Bauer, N. A. Frederick, P.-C. Ho, V. S. Zapf, and M. B. Maple, *Phys. Rev. B* **65**, 100506(R) (2002).
  - <sup>9</sup> M. Imai, M. Akaishi, E. H. Sadki, T. Aoyagi, T. Kimura, and I. Shirovani, *Phys. Rev. B* **75**, 184535 (2007).
  - <sup>10</sup> I. Shirovani, S. Sato, C. Sekine, K. Takeda, I. Inagawa, and T. Yagi, *J. Phys.: Condens. Matter* **17**, 7353 (2005).
  - <sup>11</sup> E. Bauer, A. Grytsiv, X.-Q. Chen, N. Melnychenko-Koblyuk, G. Hilscher, H. Kaldarar, H. Michor, E. Royanian, G. Giester, M. Rotter, et al., *Phys. Rev. Lett.* **99**, 217001 (2007).
  - <sup>12</sup> R. Gumeniuk, W. Schnelle, H. Rosner, M. Nicklas, A. Leithe-Jasper, and Yu. Grin, *Phys. Rev. Lett.* **100**, 017002 (2008).
  - <sup>13</sup> D. Kaczorowski and V. H. Tran, *Phys. Rev. B* **77**, 180504(R) (2008).
  - <sup>14</sup> V. H. Tran, D. Kaczorowski, W. Müller, and A. Jezierski, *Phys. Rev. B* **79**, 054520 (2009).
  - <sup>15</sup> R. Gumeniuk, H. Rosner, W. Schnelle, M. Nicklas, A. Leithe-Jasper, and Yu. Grin, *Phys. Rev. B* **78**, 052504 (2008).
  - <sup>16</sup> J. J. Yeh and I. Lindau, *At. Data Nucl. Data Tables* **32**, 1 (1985).
  - <sup>17</sup> K. Koepf and H. Eschrig, *Phys. Rev. B* **59**, 1743 (1999).
  - <sup>18</sup> J. P. Perdew and Y. Wang, *Phys. Rev. B* **45**, 13244 (1992).
  - <sup>19</sup> M. Kohout, *Int. J. Quantum Chem.* **97**, 651 (2004).
  - <sup>20</sup> A. Ormeci, H. Rosner, F. R. Wagner, M. Kohout, and Yu.

- Grin, J. Phys. Chem. A **110**, 1100 (2006).
- <sup>21</sup> M. Kohout, *Basin, version 4.7* (2008).
- <sup>22</sup> R. F. W. Bader, *Atoms in Molecules: A Quantum Theory* (Oxford University Press, New York, 1990).
- <sup>23</sup> J. Gegner, T. C. Koethe, H. Wu, Z. Hu, H. Hartmann, T. Lorenz, T. Fickenscher, R. Pöttgen, and L. H. Tjeng, Phys. Rev. B **74**, 073102 (2006).
- <sup>24</sup> J. Gegner, H. Wu, K. Berggold, C. P. Sebastian, T. Har-  
mening, R. Pöttgen, and L. H. Tjeng, Phys. Rev. B **77**,  
035103 (2008).
- <sup>25</sup> N. Franco, J. E. Klepeis, C. Bostedt, T. van Buuren,  
C. Heske, O. Pankratov, T. A. Callcott, D. L. Ederer, and  
L. J. Terminello, Phys. Rev. B **68**, 045116 (2003).
- <sup>26</sup> B. I. Lundqvist, Phys. kondens. Materie **9**, 236 (1968).
- <sup>27</sup> S. Doniach and M. Sunjic, J. Phys. C **3**, 285 (1970).
- <sup>28</sup> S. Hufner and G. K. Wertheim, Phys. Rev. B **11**, 678  
(1975).